

CO J=1-0 observations of molecular gas interacting with galactic supernova remnants G5.4-1.2, G5.55+0.32 and G5.71-0.08 [★]

H. S. Liszt

National Radio Astronomy Observatory, 520 Edgemont Road, Charlottesville, VA, USA 22903-2475

received March 25, 2022

ABSTRACT

Context. The field just West of the galactic supernova remnant W28 ($l=6.4^\circ$, $b=-0.2^\circ$) harbors 3 of 5 newly-discovered 1720 OH maser spots and two recently-discovered candidate supernova candidates (one of which is a γ -ray source), as well as several compact and classical HII regions.

Aims. To show the interaction of radio supernova remnants with ambient molecular gas in sky field just West of W28.

Methods. We analyze a datacube of CO J=1-0 emission having $1'$ and 1 km s^{-1} resolution, made with on-the-fly mapping over the region $5^\circ \leq l \leq 6^\circ$, $-1^\circ \leq b \leq 0.5^\circ$

Results. Extended and often very bright CO emission was detected at the velocities of the 1720 MHz OH masers and around the supernova remnant G5.55+0.32 which lacks a maser. A new bipolar outflow which is marginally resolved at $1'$ resolution and strong in CO (12K) was detected at the periphery of G5.55+0.32, coincident with an MSX source; there is also a bright rim of CO just beyond the periphery of the radio remnant. The OH maser near G5.71-0.08 lies on a shell of strongly-emitting molecular gas (up to 20K). At the -21 km s^{-1} velocity of G5.4-1.2, CO covers much of the field but is weak (3 K) and undisturbed near the remnant. The extended molecular gas around the compact H II region and outflow in G5.89-0.39 (W28A2) is shown for the first time.

Key words. interstellar medium – molecules

1. Introduction.

Luminous early-type stars exert strong influence over the galactic interstellar medium (ISM) at all phases of their evolution, whether as outflows from the protostar, winds and sources of ionizing photons from the main-sequence object, or as radiative and mechanical drivers in the end-stage supernova remnant (SNR). In a few cases, the end-stage interaction of an SNR with molecular gas in the ambient ISM is apparent and these special cases have been studied with great interest; particular examples include IC443 and W44 (Denoyer, 1979, 1983), W28 (Wootten, 1981; Denoyer, 1983; Arikawa et al., 1999; Aharonian, 2008), Vela (Moriguchi et al., 2001) and others noted by Arikawa et al. (1999), Reynoso & Mangum (2000) and Moriguchi et al. (2005)

Study of the SNR-ISM interaction has been hindered by the relative paucity of identified SNR compared with accepted rates of star death and by the absence of large-scale, high-resolution surveys of the OH 1720 MHz and CO emission which are typically used to trace the interaction. However, new

radiocontinuum surveys of the galactic plane (Helfand et al., 2006; Brogan et al., 2006) have recently identified a host of (candidate) SNR in the inner galaxy and surveys searching for signposts of interaction in the 1720 MHz transition of OH have been conducted by Hewitt & Yusef-Zadeh (2009).

The sky just to the galactic West of W28 (G6.4-0.2) is particularly interesting in this context because two new candidate SNR were noted by Brogan et al. (2006) and searches of these objects returned 3 of only 5 newly-detected 1720 MHz OH maser spots (out of 35 fields searched) in the work of Hewitt & Yusef-Zadeh (2009). Moreover, the field is a copious HESS source of γ -rays coincident with several SNR and the nearby molecular gas mapped in CO with $4'$ resolution at NANTEN (Aharonian, 2008). Also in the field is the very bright ultra-compact HII region G5.89-0.39 (W28-A2) with a well-studied molecular outflow (Klaassen et al., 2006; Stark et al., 2007; Watson et al., 2007; Hunter et al., 2008).

By chance, the field west and south of W28 was recently mapped at comparatively high resolution ($1'$) in CO J=1-0 emission for other purposes, namely to show the intake and shredding of gas into the galactic dust lane running along the large-scale galactic bar (Liszt, 2006). As a result, only the high-velocity portion of the emission and the more westerly portion of the field were discussed. However, the full datacube con-

Send offprint requests to: H. S. Liszt

[★] Based on observations obtained with the ARO Kitt Peak 12m telescope.

Correspondence to: hliszt@nrao.edu

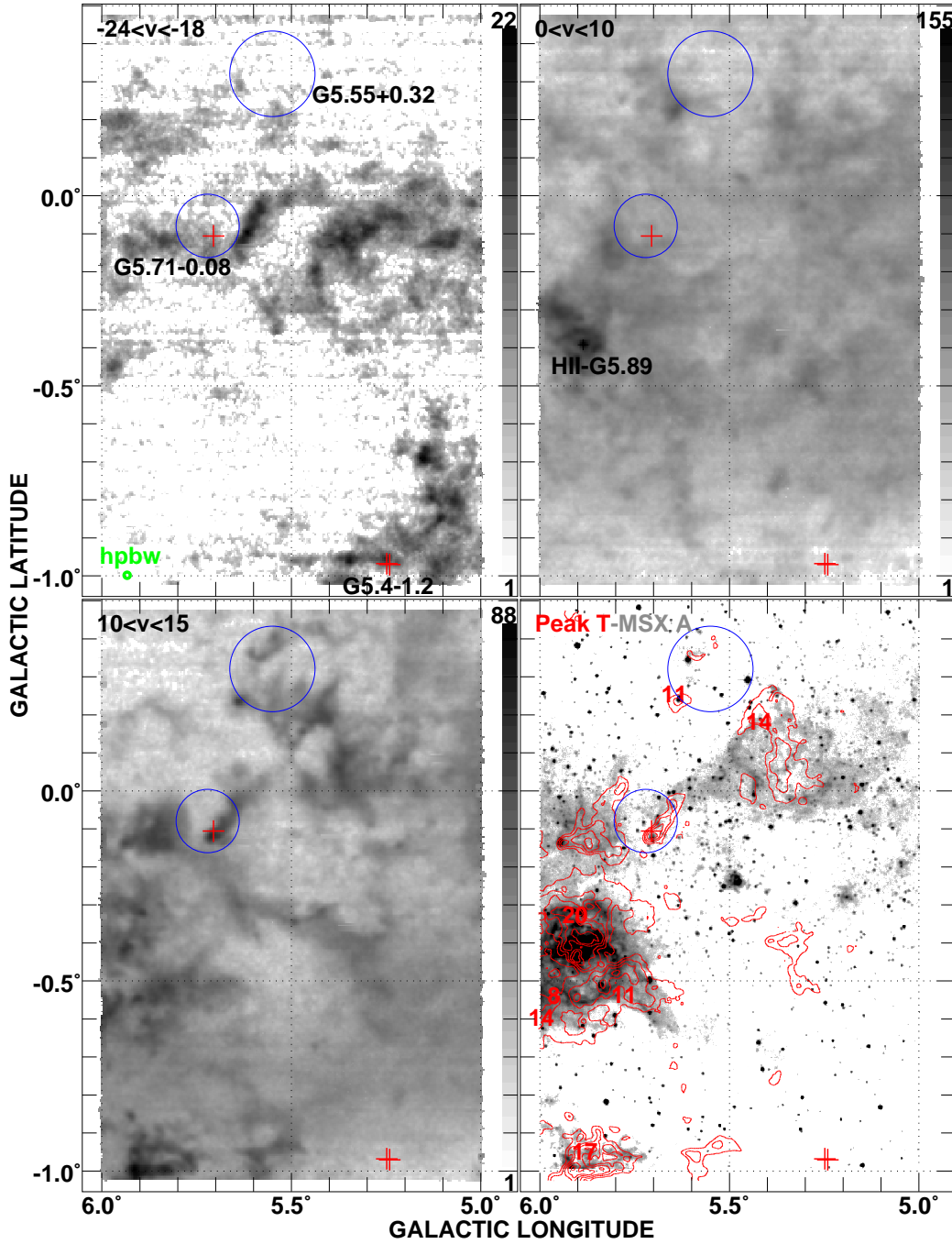


Fig. 1. CO J=1-0 and MSX 8.3 μ IR emission in the field around $l=5.5^\circ$. In the panel at lower right, a map of the peak CO temperature at $|v| < 26 \text{ km s}^{-1}$ is shown as (red) contours of temperature in Kelvins at levels 8,11,14,17,20 K superposed on an image of MSX Band A emission around 8.3 μ . In the other panels, the grey scale represents CO emission (W_{CO}) integrated over the velocity ranges indicated in each panel and the bar scales show the gradation of intensity and the peak integrated line brightness W_{CO} . The 1' ARO 12m telescope HPBW is shown in the upper left panel. Crosses (red) mark the positions of three newly-detected 1720 MHz OH maser spots (Hewitt & Yusef-Zadeh, 2009) and the outlines of two new SNR “candidates” discovered by Brogan et al. (2006) are sketched as (blue) circles.

tains a wealth of information on the molecular gas, HII regions and SNR in the more nearby regions of the Galaxy, and this is discussed here for the first time.

The organization of this paper is as follows. Section 2 summarizes the CO datacube. Section 3 shows the sky in this region and Section 4 is a brief summary.

2. The data and nominal conversion to H₂ mass

The CO datacube which forms the basis of this work was presented originally by Liszt (2006) and can now be obtained from the SIMBAD site. [NB: SIMBAD tells me that they will host the cube if the paper is published, for now the cube maybe downloaded from <ftp://tinyurl.com/ftphsl/broad5co.flb>]

The region $5^\circ \leq l \leq 6^\circ$, $-1^\circ \leq b \leq 0.5^\circ$ was mapped at the ARO 12m telescope on several successive days in 2002 May in on-the-fly mode, resulting in a map which is fully sampled in space at $1'$ resolution on a $15''$ pixel grid, with channel spacing 390.6 kHz or 1.016 km s⁻¹ and slightly lower resolution, 1.2 km s⁻¹. The single-channel rms noise level is typically 0.25 K. The brightness scale of the ARO 12m telescope is on the T_r^* scale and $T_{mb} \approx T_r^*/0.85$. All CO brightnesses quoted here are on the native T_r^* scale and all velocities are with respect to the Local Standard of Rest.

Nominal H₂ masses associated with the CO emission are calculated assuming a typical conversion factor $N(\text{H}_2) = 2 \times 10^{20}$ cm⁻² W_{CO} where W_{CO} is an integrated brightness of CO in units of K-km s⁻¹.

3. Disk and bar gas near the galactic plane at 5°

$< l < 6^\circ$

The sky is shown in the four panels of Fig. 1 and illustrative profiles at four pixels are shown in Fig. 2. The galactic coordinates of the pixels are shown in each of the panels of Fig. 2.

In Fig. 1 the positions and approximate extent of the SNR G5.55+0.32 and G5.71-0.08 are illustrated by (blue) circles; the presence of SNR G5.4-1.2 is noted at the bottom of the upper left panel but the body of the remnant lies outside these images. W28 lies 0.4° East of the left edge of these maps. The new 1720 MHz OH maser spots discovered by Hewitt & Yusef-Zadeh (2009) are shown as (red) crosses and the $1'$ telescope beam (hpbw) is shown in the upper left panel. The HII region W28A2 = G5.89-0.39 is noted in the upper right panel. Another, much larger and brighter H II region and strong MSX source at $l=6^\circ$, $b=-1.2^\circ$ is not apparent in Fig. 1 but it extends into the lower left corner of the mapped region and is responsible for the very bright CO which is found there (see the lower panels).

Except at lower right, the panels show CO emission integrated over velocity ranges chosen to contain a 1720 OH maser or other aspect; the range is indicated at upper left in each panel and the integrated brightness levels (W_{CO}) are indicated by the bar scale. The panel at lower right shows (red) contours of the peak CO brightness over the wider range -26 km s⁻¹ $< v < 26$ km s⁻¹ overlaid on an image of MSX (Price et al., 2001) Band A 8.3μ emission.

3.1. G5.4-1.2

Two of the new OH maser spots found by Hewitt & Yusef-Zadeh (2009) occur in the lower right portion of our maps but the CO line in the region is entirely undistinguished, see Fig. 2 at lower right. CO emission

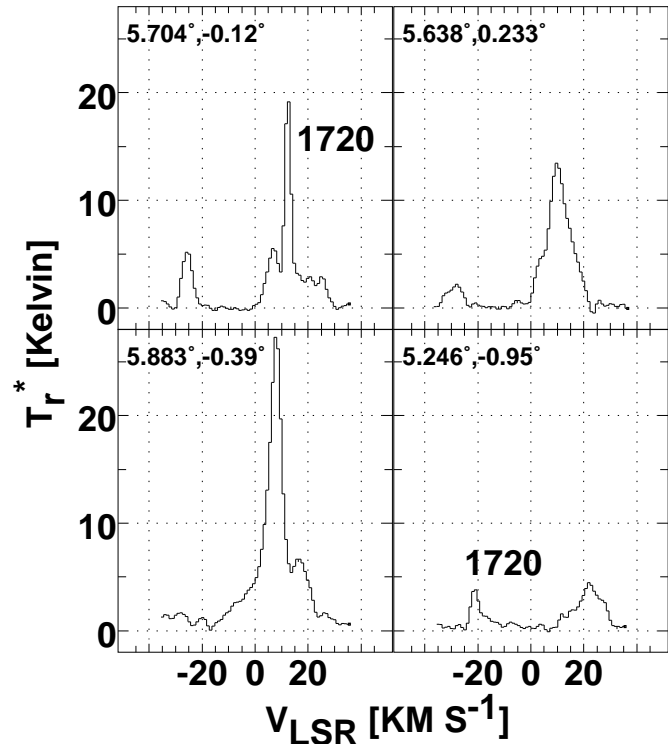


Fig. 2. ARO ¹²CO profiles at 4 pixels in Fig. 1. Galactic coordinates are indicated in each panel. The channel spacing is 1.016 km s⁻¹ (resolution 1.2 km s⁻¹) and the spatial resolution is $1'$.

around -21 km s⁻¹ is very widespread and vertically extended. As noted by Hewitt & Yusef-Zadeh (2009) this velocity is inconsistent with normal rotation in the galactic disk but corresponds approximately to that of the extended 3 kpc arm (Bania, 1980) which lies interior to the galactic molecular ring, within the large-scale galactic bar (Fux, 1999); the 3 kpc arm is not otherwise understood to be so broad in latitude. No especially strong CO emission from gas at this velocity is found anywhere in Fig 1 (compare the upper left and lower right panels) but perhaps a yet-larger scale map would find clearer evidence of the SNR-neutral gas interaction in CO further to the South. At a distance of 5 kpc the nominal H₂ mass of the entirety of the -21 km s⁻¹ gas at $l < 5.4^\circ$, $b < -0.6^\circ$ is $1.2 \times 10^4 M_{\text{sun}}$,

3.2. G5.55+0.32

No maser spot was detected around this source by Hewitt & Yusef-Zadeh (2009) but strong (14K) CO emission is found at G5.64+0.23 (Fig. 2) near the periphery of the remnant, along with a ± 9 km s⁻¹ outflow which is marginally spatially resolved at our $1'$ resolution. As seen in the lower right panel of Fig. 1 there is an MSX source coincident with the CO peak and outflow, and it is especially prominent in its field in MSX Band E at 22μ (not shown here).

Is there a shell of neutral gas around the SNR G5.55+0.32? Perhaps a better question is where a candidate shell is not found in Fig. 1. However, to the galactic south and southwest there is

a very bright (peak 15 K) CO rim at $v = 10\text{--}15 \text{ km s}^{-1}$ just outside and seemingly tangent to the cartoon outline of the SNR (which is exceedingly faint and diffuse in the radiocontinuum). Although in only in the very brightest or most kinematically or chemically disturbed gas will it be possible to establish an association in such a complicated region, such bright CO is seldom if ever seen in quiescent ambient dense gas in the general ISM. At a distance of 2 kpc the nominal mass of H_2 in the bright rim SW of the SNR is $3 \times 10^3 M_{\text{sun}}$; within a circle of radius $0.2''$ inscribed about the SNR the nominal mass is $1 \times 10^4 M_{\text{sun}}$.

3.3. G5.71-0.08

This SNR (Brogan et al., 2006) coincides with γ -ray source HESSJ1800-240C and molecular emission at $0\text{--}20 \text{ km s}^{-1}$ near and just East of it (at $l \approx 5.8^\circ$) was shown with much lower resolution NANTEN CO data ($2.7'$ beam sampled at $4'$ intervals) by Aharonian (2008).

The peak CO temperature map at lower right in Fig. 1 shows that there is a rim of bright CO emission around the SNR G5.71-0.08, with a rather narrow and very bright (19 K) CO line (Fig. 2) at the 12 km s^{-1} 1720 MHz OH maser velocity, immediately adjacent to the maser spot. Gas in the rim to the east of the remnant shows strong positional velocity gradients, with more positive velocity (and velocities above 15 km s^{-1}) to the north and west, which accounts for the fact that a shell is more visible in the peak temperature map.

All of the gas at $10\text{--}15 \text{ km s}^{-1}$ southeast of G5.71 is bright, as outlined in the peak temperature map at lower right in Fig. 1. To the southeast, just outside the bright rim there, is a very bright compact peak centered at G5.88,-0.13 and it is this gas which appears in the NANTEN CO map shown by Aharonian (2008). The bright CO in the western rim of the shell near the 1720 OH maser in our data is not apparent in the representation of the NANTEN data shown by Aharonian (2008).

A careful search of the CO profiles in this region did not show clear instances of the sort of broad-lined emission which sometimes characterizes shocked molecular gas, for instance in IC443 (Denoyer, 1979), at least in part because of seeming confusion with other kinematic components; the broader weaker emission at $0\text{--}30 \text{ km s}^{-1}$ around the bright narrow 12 km s^{-1} feature at G5.704-0.12 in Fig. 2 is broadly-distributed on the sky. Denoyer (1983) noted the difficulty of finding such evidence in a region as kinematically complicated as the galactic plane around $l=6^\circ$, but shocked molecular gas near W28 was later found in more complete mapping at higher resolution by Arikawa et al. (1999).

As shown by the $v = -21 \text{ km s}^{-1}$ CO near the OH maser spot around the SNR G5.4-1.2, CO lines are by no means always bright in gas around SNR, even when an interaction is occurring (Arikawa et al., 1999). However, bright CO seems to be the rule in W28 and in the SNR nearest to it in the region surveyed here. The presence of such bright CO lines is always the result of some special interaction, but whether that interaction is with the SNR or one of the H II regions is a matter for further discussion.

At a distance of 2 kpc the nominal H_2 mass in the ridge of bright 12 km s^{-1} emission containing the 1720 OH maser spot is $2 \times 10^3 M_{\text{sun}}$ and a circle inscribed about the SNR which includes this ridge and the gas west of the SNR encloses $4 \times 10^3 M_{\text{sun}}$. Including all of the bright gas to the east increases the mass to $7 \times 10^3 M_{\text{sun}}$.

3.4. G5.89-0.39 and other thermal sources

Figure 3 shows in greater detail the distribution of CO and IR emission in the vicinity of the HII region W28A2 = G5.89-0.39. The well-studied bipolar outflow is visible in our data at the marked location but unresolved. Neglecting the outflow, CO emission associated with the body of W28A2 occurs mostly at $v \lesssim 10 \text{ km s}^{-1}$ and the strong emission at $b = -0.125^\circ$ just north of W28 in the panel of Fig. 3 centered at 13 km s^{-1} is actually a distinct kinematic system which probably represents a separate H II region near the $+12 \text{ km s}^{-1}$ velocity of the 1720 MHz OH maser spot.

The nominal H_2 mass of the molecular gas overlaying the body of W28A2 and interior to the pseudo-shell shown in the lower right panel of Fig. 3 is $2 \times 10^4 M_{\text{sun}}$.

4. Summary

We discussed CO J=1-0 emission observed by the ARO Kitt Peak 12m telescope with $1'$ and 1 km s^{-1} resolution in the region $5^\circ < l < 6^\circ$, $-1.0^\circ < b < 0.5^\circ$, just west of the SNR W28. The mapped region contains the compact HII region W28A2 (G5.89-0.39) and other more diffuse thermal ionized gas (as seen at mid-IR wavelengths in MSX data), several candidate SNR (one of which, G5.71-0.08 is coincident with the γ -ray source HESS J1800-240C) and several newly-discovered 1720 MHz OH maser spots signifying interaction between SNR and ambient molecular gas. The region is also host to a wide variety of behavior in the CO emission, including a newly-discovered outflow source and very bright CO emission associated with both the thermal and non-thermal compact sources.

We showed the CO J=1-0 emission at the velocities of three newly-discovered 1720 MHz OH maser spots. At -21 km s^{-1} CO, associated with G5.4-1.2, CO emission is widespread and emission near the maser is weak (3 K) and mundane. By contrast, CO emission around the other two SNR in the region is stronger and more remarkable. There is a bright (14 K) newly-detected CO outflow source near G5.55+0.32 (which lacks a maser) and a rim of strong (15 K) CO emission just outside the remnant. CO emission at the OH maser spot toward G5.71-0.08 is extremely strong (19 K) and arcs of bright CO emission are seen around most of the periphery of this SNR. Typical masses of the molecular clouds around the SNR are $10^4 M_{\text{sun}}$.

A concentration of strong CO just east of G5.71-0.08, previously observed in a low-resolution NANTEN map on a $4'$ pixel grid, overlays diffuse thermal (MSX) emission and an MSX point source at $l=5.9^\circ$, $b=-0.13^\circ$ which is probably the exciting source of a separate, classical HII region seen just north of the stronger thermal source W28A2, G5.89-0.39. Molecular gas associated with the compact outflow source in G5.89-0.39 has been widely discussed but the larger-scale distribution of

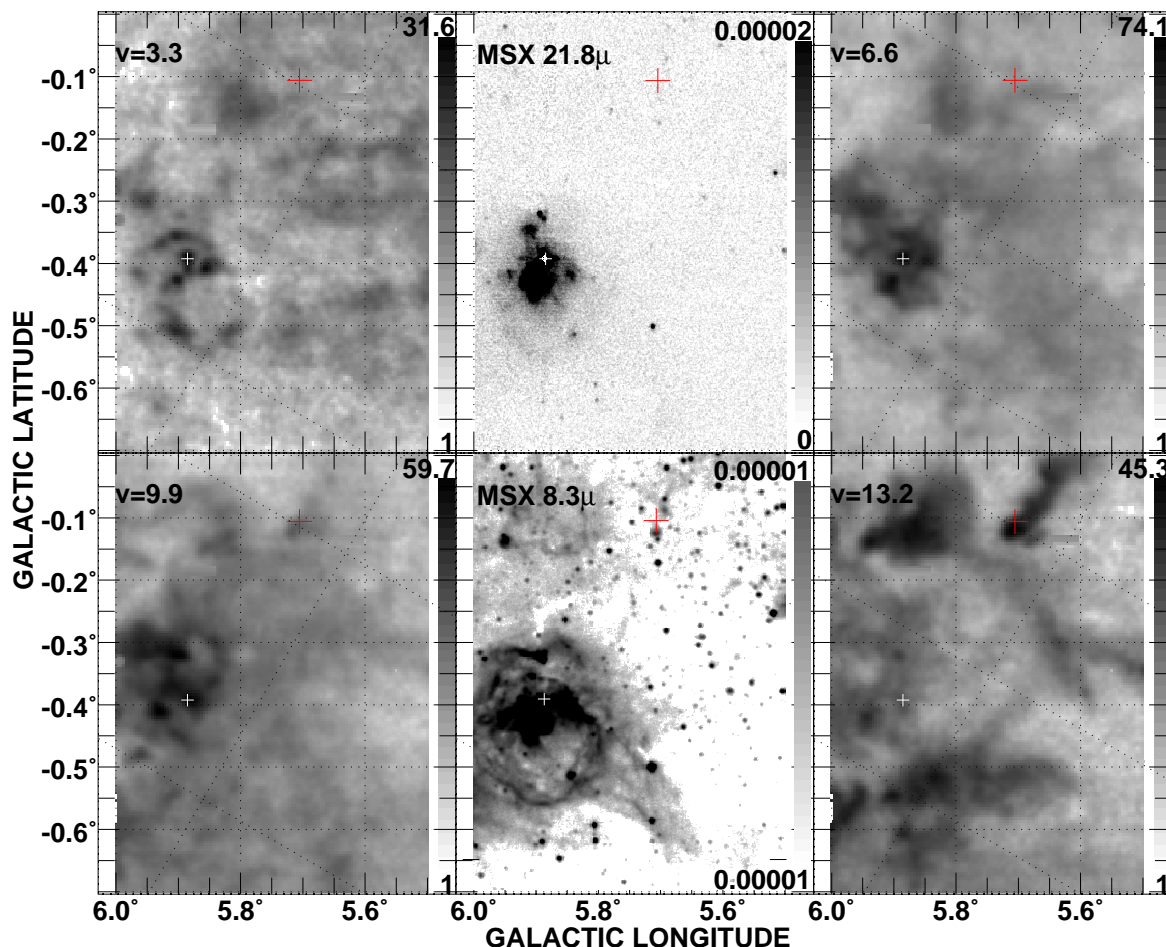


Fig. 3. ARO CO and MSX IR maps of W28A2 (G5.89-0.39) and its surroundings. The middle panels show MSX Band A (bottom) and E (top) IR emission, while the outer panels show integrated brightness of CO J=1-0 over 3-channel wide (3.047 km s^{-1}) intervals centered at the indicated velocities. The position of the 1720 MHz OH maser discovered by Hewitt & Yusef-Zadeh (2009) is marked by the upper (red) cross.

CO emission around this HII region was shown in detail here for the first time. It does not show any obvious sign of having been influenced by interaction with the outflow.

The profusion of compact thermal and non-thermal sources, thermal ionized gas and molecular clouds in the region presents an opportunity for study of the interaction between various phases of stellar evolution and the ISM, and indeed further study will be required to understand, as it were, just who is doing what to whom, and with what.

Acknowledgements. The National Radio Astronomy Observatory is operated by Associated Universities, Inc. under a cooperative agreement with the US National Science Foundation. The Kitt Peak 12-m millimetre wave telescope is operated by the Arizona Radio Observatory (ARO), Steward Observatory, University of Arizona. I am grateful to the ARO Director, Dr. Lucy Ziurys, for awarding the observing time necessary to perform these observations and to the ARO staff and 12m operators who keep the telescope running at such a laudably high level.

References

- Aharonian, F. 2008, *A&A*, 481, 401
- Arikawa, Y., Tatematsu, K., Sekimoto, Y., & Takahashi, T. 1999, *Publ. Astron. Soc. Jpn.*, 51, L7
- Bania, T. M. 1980, *ApJ*, 242, 95
- Brogan, C. L., Gelfand, J. D., Gaensler, B. M., Kassim, N. E., & Lazio, T. J. W. 2006, *ApJ*, 639, L25
- Denoyer, L. K. 1979, *ApJ*, 232, L165
- . 1983, *ApJ*, 264, 141
- Fux, R. 1999, *A&A*, 345, 787
- Helfand, D. J., Becker, R. H., White, R. L., Fallon, A., & Tuttle, S. 2006, *Astron. J.*, 131, 2525
- Hewitt, J. W. & Yusef-Zadeh, F. 2009, *ApJ*, 694, L16
- Hunter, T. R., Brogan, C. L., Indebetouw, R., & Cyganowski, C. J. 2008, *ApJ*, 680, 1271
- Klaassen, P. D., Plume, R., Ouyed, R., von Benda-Beckmann, A. M., & Di Francesco, J. 2006, *ApJ*, 648, 1079
- Liszt, H. S. 2006, *A&A*, 447, 533
- Moriguchi, Y., Tamura, K., Tawara, Y., Sasago, H., Yamaoka, K., Onishi, T., & Fukui, Y. 2005, *ApJ*, 631, 947
- Moriguchi, Y., Yamaguchi, N., Onishi, T., Mizuno, A., & Fukui, Y. 2001, *Publ. Astron. Soc. Jpn.*, 53, 1025
- Price, S. D., Egan, M. P., Carey, S. J., Mizuno, D. R., & Kuchar, T. A. 2001, *Astron. J.*, 121, 2819

- Reynoso, E. M. & Mangum, J. G. 2000, *ApJ*, 545, 874
- Stark, D. P., Goss, W. M., Churchwell, E., Fish, V. L., & Hoffman, I. M. 2007, *ApJ*, 656, 943
- Watson, C., Churchwell, E., Zweibel, E. G., & Crutcher, R. M. 2007, *ApJ*, 657, 318
- Wootten, A. 1981, *ApJ*, 245, 105